



CATALYTIC BEHAVIOUR OF NEODYMIUM SUBSTITUTED ZINC FERRITES IN OXIDATIVE COUPLING OF METHANE

Florica PAPA,* Luminița PATRON, Oana CARP, Carmen PARASCHIV and Ioan BALINT

Institute of Physical Chemistry of the Roumanian Academy, Spl. Independentei 202, 060021 Bucharest, Roumania

Received November 11, 2008

The catalytic behavior for oxidative conversion of methane, oxidative coupling of methane was investigated for the first time over pure and neodymium substituted zinc ferrites prepared by combustion method. The catalytic activity proved to be strongly related to the oxide structure as well as to the specific defects created by substitution. The pure zinc ferrite (ZnFe_2O_4) and ZnNd_2O_4 exhibited high activity for coupling reaction whereas the neodymium substituted ferrites ($\text{ZnFe}_{1.75}\text{Nd}_{0.25}\text{O}_4$, $\text{ZnFe}_{1.5}\text{Nd}_{0.5}\text{O}_4$ and ZnFeNdO_4) was low active in this reaction. The catalytic activity of the oxides and the reaction mechanism on simple and mixed oxides is discussed in light of the experimental results.

INTRODUCTION

The *oxidative coupling of methane* (OCM) may prove to be a viable alternative to obtaining higher hydrocarbons starting from methane, which is a relatively cheap and abundant raw material. Due to the great practical impact, the OCM reaction was intensively investigated. The catalytic activity of a broad class of simple and mixed oxides as well as of supported metals has been already investigated. Several reviews have been dedicated to the oxidative conversion of methane over simple and mixed oxides.^{1,2}

However, in the spite of the intense research there is still enough room for improvements in catalytic performances as well as in stability to obtain ideally tuned materials for a specific practical application.

The catalytic activity of pure, Zr and Sr doped Nd_2O_3 for OCM reaction was already reported.^{3,4} The yield to C_2^+ over these materials was relative modest, remaining below 15%. Ferrites have been investigated up now much more for their interesting magnetic properties. However, the catalytic activity of ZnFe_2O_4 for oxidative dehydrogenation of n-butene.^{5,6} Thus, study of the methane oxidative conversion over simple and Nd substituted zinc ferrite (ZnFe_2O_4) would be a novelty in the catalytic field. The catalytic activity of the ZnNd_2O_4 , having an ordered crystalline structure of K_2NiF_4 type, is

also reported here for the first time. As we shall show later, Nd_2ZnO_4 can be a very promising starting material for a novel class of OCM catalysts showing high selectivity to C_2 hydrocarbons as well as high stability in reaction conditions.

The aims of our investigation were (i) to investigate the catalytic behavior of the pure and neodymium doped zinc ferrites for oxidative coupling of methane, (ii) to observe the effect of Fe^{3+} substitution by Nd^{3+} on the catalytic behavior for oxidative conversion of methane in oxygen poor (OCM) atmospheres, (iii) to get a better understanding on the generation, nature and role of lattice defects on the catalytic reactivity.

EXPERIMENTAL

The principle of the preparation procedure consisted in the use of metal coordination compounds as precursors of the final mixed oxides.^{7,8} The $\text{ZnFe}_{2-x}\text{Nd}_x\text{O}_4$ ($x = 0, 0.25, 0.5, 0.75$ and 1.0) type mixed oxides were prepared starting from the tartarate complexes of the constituent metals.

The solutions containing the mixtures of complex metal tartarates were slowly heated and kept at 80°C for 1h. After cooling to room temperature, ethanol was added and then the pH was adjusted to 5.5 – 6 by using a solution of ammonia in ethanol (1:1). The resulted light-yellow precipitate was maintained in liquid phase at 4°C for 24 h, filtered, washed several times with a mixture of ethanol and water and finally dried on P_4O_{10} . The final step consisted in the air calcination of the precipitates at 800°C for 1 h.

* Corresponding author: frusu@icf.ro

Activity tests for OCM reactions were performed at atmospheric pressure with 0.1 g of catalyst (0.3 - 0.8-mm fraction) loaded in a tubular quartz microreactor (i.d. = 8 mm). The blank tests in O₂/CH₄ reactant mixtures with the reactor containing only quartz wool revealed that the homogeneous conversion of CH₄ started from T > 850 °C, which was the highest temperature of our study. The reactor was heated with a furnace connected to a temperature controller (Shimaden, Model SR 25). The reactant gaseous mixtures were prepared using electronic flow controllers (Aalborg). The typical total flow rates of the reaction mixtures for OCM reaction were 24 cm³/min STP (standard temperature and pressure). The corresponding GHSV (gas hourly space velocity) were 14400 h⁻¹. The composition of reaction mixtures for OCM reaction were 41.6% CH₄, 8.4% O₂ (CH₄/O₂ = 5/1) in Ar. The gaseous mixtures (O₂, CH₄, CO₂, C₂H₆ and C₂H₄) to and from the reactor were analyzed with a Buck Scientific gas chromatograph equipped with TCD detectors.

Temperature programmed reduction (TPR) experiments were carried out in a flow system, with 0.1 g of catalyst, by using a Chembet 3000-Quantachrome Instruments type apparatus equipped with thermal conductivity detectors (TCD). The gas mixture used in TPR measurements was 3% H₂ in Ar. The typical heating rate was 10 °C/min⁻¹ and the total flow rate of the oxidizing or reducing gaseous mixtures was 70 ml min⁻¹. A silicagel water trap was interposed

between the analyzed sample and the TCD detector in order to ensure a good stability and sensitivity of the detection system.

The crystalline structure of the prepared samples was analyzed with a Rigaku Multiflex diffractometer provided with peak assignment software using Cu K α radiation ($\lambda = 1.54050 \text{ \AA}$) at 0.02 °/s step.

RESULTS

At $x = 0$, the oxide (ZnFe₂O₄) exhibits a cubic structure, which is typical for spinels (see Fig. 1a). The tetrahedral sites of the cubic structure are occupied by zinc ions ($r = 0.6 \text{ \AA}$) whereas the octahedral ones by iron ions. As can be seen from X-ray diffraction Fig. 2, the substitution of Fe³⁺ ($r = 0.87 \text{ \AA}$) by Nd³⁺ ($r = 1.16 \text{ \AA}$) determines a gradual change in the crystalline structure from cubic to orthorhombic one.

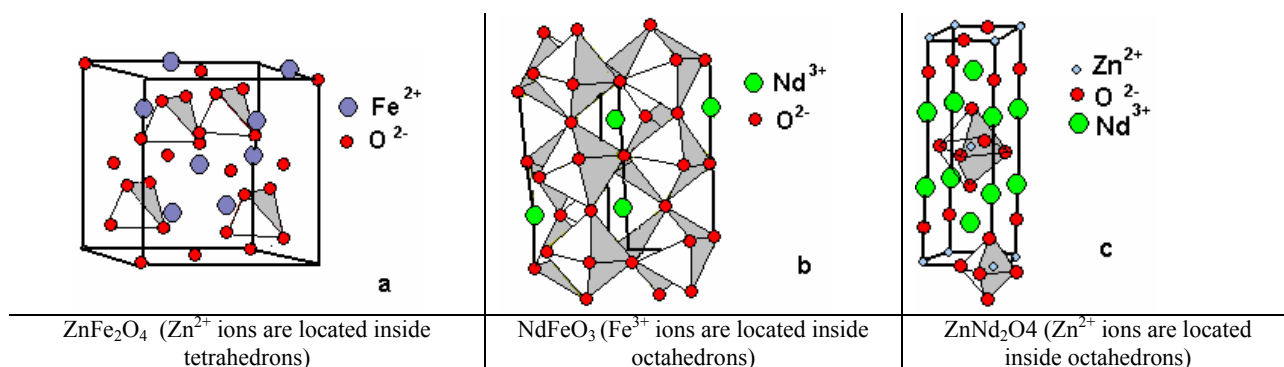


Fig. 1 – The crystalline structure of ZnFe₂O₄ (spinel type), NdFeO₃ (perovskite type) and ZnNd₂O₄ (K₂NiF₄ type).

Thus, in the Nd substituted ferrites (ZnFe_{1.75}Nd_{0.25}O₄, ZnFe_{1.5}Nd_{0.5}O₄ and ZnFeNdO₄) the initial cubic phase of the pure zinc ferrite coexisted with the newly formed orthorhombic phase of NdFeO₃ (see Fig. 1 b). The formation of the NdFeO₃ secondary phase can be explained by the limited solubility of voluminous Nd³⁺ ions in the host spinel lattice. An oxide having a distorted tetragonal K₂NiF₄ structure (fig.1 c) was obtained for a substitution of $x=2$ (ZnNd₂O₄). This structure is formed by (ZnO₂)²⁻ and (Nd₂O₂)²⁺ alternating units in which Nd³⁺ and Zn²⁺ ions are surrounded by 8 and 4 O²⁻, respectively.⁹ It should be emphasized that, the presence of ZnNd₂O₄ phase was not observed in the substitutes ferrites.

The physical surface area (BET) of the oxides calcined at 800 °C is relatively small, ranging between 6.2 and 14.9 m² g⁻¹ (see Table 1). As expected, the specific hydrogen consumption in TPR runs decreased with the decreasing in the amount of reducible iron in the mixed oxide.

The hydrogen consumption in the case of ZnNd₂O₄ was negligible as both zinc and neodymium have only one stable oxidation state. Later on we shall discuss in more details the relationship between TPR results, the catalytic activity and reaction mechanism.

The catalytic activity of the simple and of the neodymium substituted ZnFe₂O₄, expressed in term of yield to C₂⁺ (ethane + ethylene), is presented in Fig. 3. Depending on the catalytic material, the temperatures corresponding to the highest yields to C₂⁺ ranged between 775 and 825 °C. One of the reasons of sharp decrease in the yield to C₂⁺ after reaching the maximum activity is the collapse of the crystalline structure in reaction conditions. After reaction, deposits of white ZnO could be observed on the reactor walls as a result of the separation from the ZnFe_{2-x}Nd_xO₄ host lattice followed by sublimation.

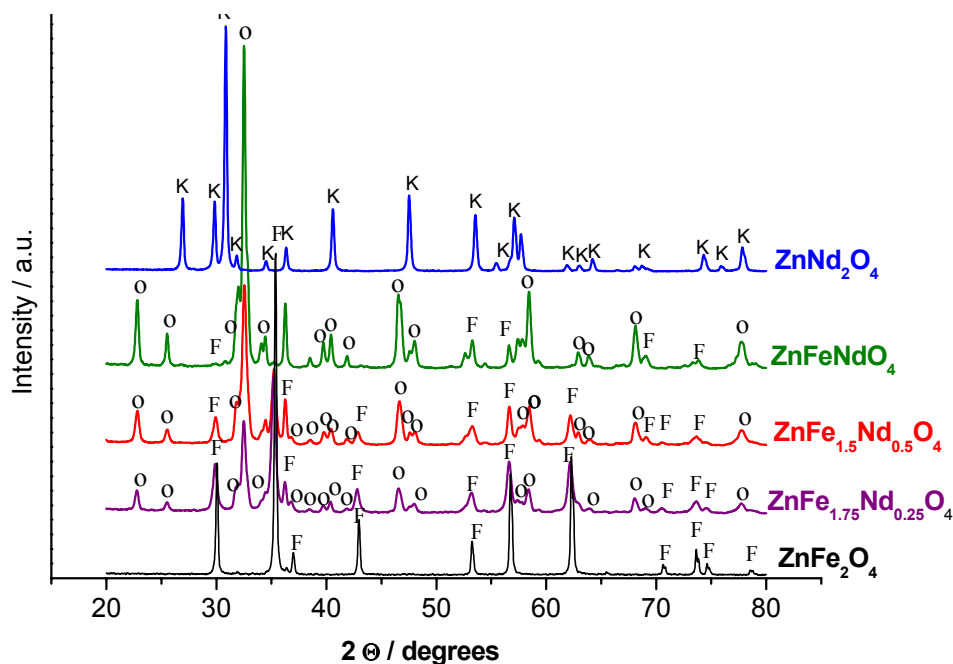


Fig. 2 – Comparative XRD spectra of neodymium substituted zinc ferrites. The peak assignments are the following: F- cubic ferrite phase; o –orthorhombic NdFeO_3 phase, K- distorted tetragonal K_2NiF_4 type structure of ZnNd_2O_4 phase.

Table 1

The physical surface area (BET) and the specific amount of H_2 consumed in the TPR runs of the investigated oxide catalysts

Catalyst	$S_{\text{BET}} / \text{m}^2 \text{g}^{-1}$	H_2 consumption / $\text{mmol g}^{-1} \text{catalyst}$
ZnFe_2O_4	6.2	4.79
$\text{ZnFe}_{1.75}\text{Nd}_{0.25}\text{O}_4$	13.5	3.38
$\text{ZnFe}_{1.5}\text{Nd}_{0.5}\text{O}_4$	14.9	2.40
ZnFeNdO_4	10.8	0.65
ZnNd_2O_4	8.1	0.01

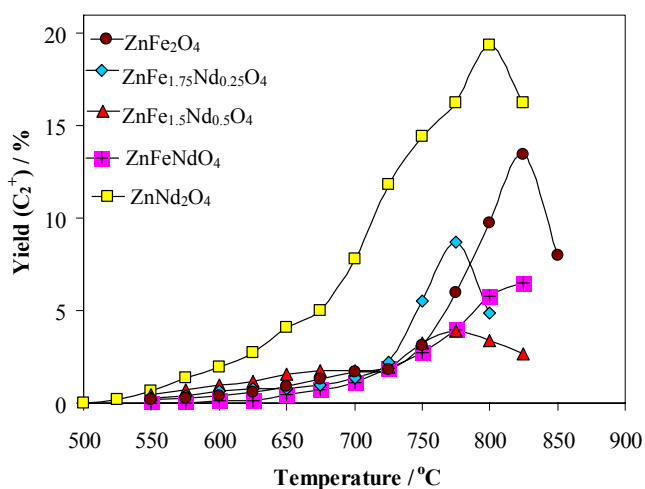


Fig. 3 – The catalytic yield to C_2^+ for OCM reaction of Nd substituted zinc ferrites as a function of reaction temperature.

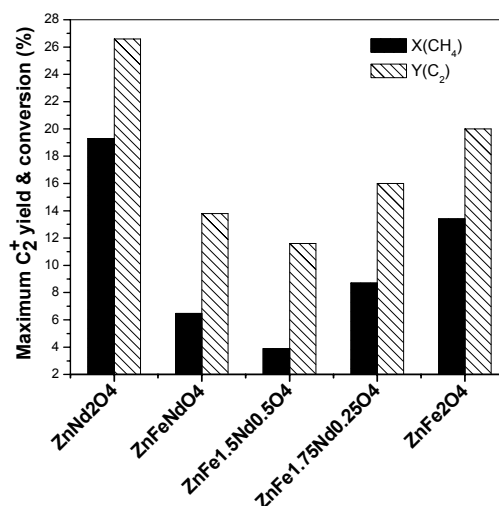


Fig. 4 – The effect of Fe^{3+} substitution with Nd^{3+} on the catalytic activity (conversion) and yield of zinc ferrites for OCM reaction.

The order of the catalytic activities expressed as yields to C_2^+ were $\text{ZnNd}_2\text{O}_4 > \text{ZnFe}_2\text{O}_4 >$

$\text{ZnFe}_{1.75}\text{Nd}_{0.25}\text{O}_4 > \text{ZnFeNdO}_4 > \text{ZnFe}_{1.5}\text{Nd}_{0.5}\text{O}_4$. As can be seen in Fig. 3, the lattice stability in

reaction conditions may have influence on the peak catalytic activity. However, the effect on the position of peak activity (see Fig. 3) should be minor as the stability of the investigated oxides resembles. The crystalline structures become unstable in reaction conditions between 775 and 825 °C. Later on we will show that, the stability of the simple and neodymium substituted ferrites, with the exception of ZnNd_2O_4 , in reducing atmosphere resembles. Similar comment can be made for the contribution of surface area to the overall reactivity of the investigated oxides. The surface areas of the catalytic oxides are relatively small, ranging between 8 and 15 $\text{m}^2 \text{g}^{-1}$ (see Table 1). The catalytic activity for OCM reaction shows a significant dependence on the degree of Fe^{3+} substitution with Nd^{3+} .

Fig. 4 shows the variation of the catalytic activity and yield to C_2^+ as a function of Fe^{3+} substitution degree with Nd^{3+} . The yield to C_2^+ and the conversion of methane exhibit the same trend. The yield to C_2^+ decreased from $\approx 13\%$ for pure ZnFe_2O_4 to $\approx 4\%$ for $\text{ZnFe}_{1.5}\text{Nd}_{0.5}\text{O}_4$ with the progressive replacement of Fe^{3+} with Nd^{3+} . Then, for higher substitution degree of Fe^{3+} with Nd^{3+} the yield to C_2^+ showed an increasing trend. The highest yield to C_2^+ of $\approx 19\%$ was observed when Fe^{3+} was completely substituted by Nd^{3+} (ZnNd_2O_4).

The analysis of the TPR profiles (see Fig. 5) can give useful information regarding the behavior

in reducing reaction mixtures. In the OCM reaction the optimum reaction temperature is located between 775 and 825 °C. Thus, the oxide catalysts are likely to be in a partial reduced state where the iron is in a mixed oxidation state ($\text{Fe}^{2+, 3+}$). The quantitative analysis of the reduction profiles, based on hydrogen consumption (see Table 1), shows that the reduction of Fe^{3+} to Fe^{2+} takes in two steps, yielding two corresponding TPR peaks. The first reduction step of Fe^{3+} to an intermediate oxidation state ($\text{Fe}^{2+, 3+}$) is taking place between 553 and 634 °C. The second step consisting in reduction of $\text{Fe}^{2+, 3+}$ to Fe^{2+} takes place at temperatures between 681 and 791 °C. The temperature of the specific reduction peaks is shifted progressively to lower values as the amount of reducible Fe^{3+} decreases as a result of its substitution with Nd^{3+} . As expected, the hydrogen consumption for ZnNd_2O_4 was negligible, 0.01 mmol g^{-1} (see Table 1). The TPR spectrum of the Fe_2O_3 reference compound presented in Fig. 5 shows also two reduction peaks. The first reduction peak ($\text{Fe}^{3+} \rightarrow \text{Fe}^{2+, 3+}$) is located at lower temperatures (495 °C) compared to the simple and to the substituted zinc ferrites where $T \geq 553$ °C. The explanation is that the Fe^{3+} located in the lattice of simple and substituted zinc ferrites is more resistant against reduction compared to that of Fe_2O_3 .

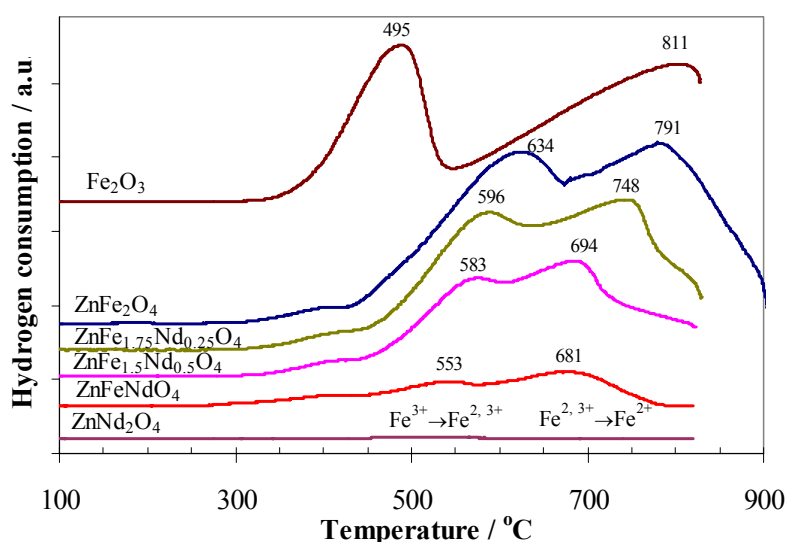


Fig. 5 – Termoprogrammed reduction of Nd substituted ZnFe_2O_4 .

DISCUSSION

In the case of oxide catalysts it is accepted that the charged surface or bulk oxygen species can

activate hydrocarbons. Based on EPR, XPS, IR and Raman evidences, several oxygen species (O^- , O_2^- , O_2^{2-}) have been proposed as active sites for the selective activation of methane in coupling

reaction.¹⁰ In contrast, the adsorbed oxygen species having a very short life time on the surface are considered responsible for the total oxidation of methane to CO₂.¹¹

In spite of the rich literature concerning the catalytic oxidation of hydrocarbons, the evolution of the structure and of the composition of oxide lattice as a function of reaction conditions is very little analyzed. Our experimental results suggest that the structure of surface and the bulk is under a permanent change, acting as a mirror of the reaction conditions. This observation is especially evident in the case of the reducible oxides. In our view, the discussion about the factors governing the catalytic behavior should focus mainly on the (i) redox behavior of the oxide in reaction mixture and (ii) effect of the doping (in our case the replacement of Fe³⁺ by Nd³⁺).

The redox behavior in reaction mixture is important because specific lattice defects are created as a result of the removal of lattice oxygen. This process is associated with the reduction of metal cation Fe³⁺). At high temperatures and in the reducing condition of OCM reaction, oxygen vacancies are likely to be created to compensate the deficit of positive charge resulted by the reduction of Fe³⁺ to Fe²⁺. The general remark is that, the working oxides are in a partially reduced state in the case of OCM reaction.

The second factor which should be analyzed more closely is the effect on the catalytic behavior of the substitution of Fe³⁺ by Nd³⁺ in the lattice of ZnFe₂O₄. An interesting characteristic of the perovskite and spinel type oxides is the possibility of varying the dimension of the unit cell by ion substitution, and thereby the covalency of the B-O bond in AB₂O₄ structure.² Moreover, the partial substitution of B-site may also affect the catalytic activity due to the stabilization of unusual oxidation states and to the simultaneous formation of structural defects. The perovskites with oxygen vacancies and mixed valency (*i. e.* Ba_{1-x}Ca_xFeO_{3-δ}) was suggested to contribute largely to the high selectivity to C₂⁺ in OCM reaction.¹² Another situation is the introduction of alkali and alkali-earth metals in B sites of LaAlO₃ to form LaAl_{1-x}M_xO₃. The substitution of Al³⁺ with Li⁺ and Mg²⁺ increased both catalytic activity and selectivity to C₂ hydrocarbons in comparison to the unsubstituted LaAlO₃ perovskites.¹³

In our specific case, the substitution of Fe³⁺ with the isoelectric Nd³⁺ does not create electrically charged lattice defects. But on the other

hand, the replacement of small Fe³⁺ (0.78 Å) with the significantly larger Nd³⁺ (1.16 Å) are likely to induce significant lattice strains along with the formation of a new crystalline phase (ZnNdO₃).

First we shall analyze the behavior of oxide catalyst in reducing conditions (excess of reductant). Both, heterogeneous and homogeneous steps are considered to be necessary for C₂ formation in OCM reaction. Our observation is that the non-doped catalysts, ZnFe₂O₄ and ZnNd₂O₄ proved to be more active for OCM reaction than the substituted zinc ferrites in B-site (ZnFe_{2-x}Nd_xO₄). On the other hand, the pure ferrite (ZnFe₂O₄) was less active than the catalyst having the cations in stable oxidation states (ZnNd₂O₄). It is known that the reducible oxides (*i. e.* ZnFe₂O₄) exhibit generally lower activity for OCM reaction compared to non-reducible oxides. The specific defects formed by iron substitution with neodymium lead to a severe decrease in catalytic activity and selectivity to C₂⁺ (see Fig. 4). In addition to the defects formed by iron substitution with neodymium, other types of defects are generated in reaction conditions (high temperatures and large methane excess) in the lattice of ZnFe₂O₄ and ZnFe_{1-x}Nd_xO₄. The formation of these defects was not beneficial for OCM reaction. The synergy between Fe and Nd may have also an important role in determining the catalytic activity and selectivity for OCM reaction.

The explanation for the observed results should take into consideration that the Fe³⁺ in the structure of zinc ferrite is undergoing under reaction conditions to a partial reduction to an intermediate oxidation state Fe^{2+ 3+} (Fe₃O₄) generating thus lattice defects. The most likely defects are oxygen vacancies which are formed to compensate the deficit of positive charges resulted by the reduction of Fe³⁺. The thermodynamic equilibrium Fe²⁺ ⇌ Fe³⁺ is shifted to left hand side in reducing conditions at high temperatures. In addition to the defects formed by iron substitution with neodymium, other types of defects are generated in reaction conditions in the lattice of ZnFe₂O₄ and ZnFe_{1-x}Nd_xO₄. The formation of these defects was not beneficial for OCM reaction. The synergy between Fe and Nd may have also an important role in determining the catalytic activity and selectivity for OCM reaction.

The highest yield to C₂⁺ of 19.3% was observed over the nonreducible ZnNd₂O₄. This catalyst showed also a stable catalytic activity in time for T ≤ 800 °C (see Fig. 5). It is likely that the

nonreducible ZnNd_2O_4 , showing little almost no redox properties, possesses a relevant amount of firmly bound lattice oxygen species which are responsible for the selective activation of methane to CH_3 . The highest yield for C_2^+ of Zr doped Nd_2O_3 was only 13%. Probable that the K_2NiF_4 type of lattice structure, assembling the Zn^{2+} and Nd^{3+} ions in an ordered manner, is also beneficial for OCM reaction.

CONCLUSIONS

The catalytic activity of simple and neodymium substituted zinc ferrites was investigated for the first time for coupling oxidative of methane (OCM) reaction. The pure ferrite (ZnFe_2O_4) and the completely substituted ferrite (ZnNd_2O_4) were the most active catalysts for OCM reaction. The redox properties of the simple and substituted ferrites as well as the nature of substitutional element were found to be important parameters in determining the catalytic behavior.

REFERENCES

1. J. S. Lee and T. Oyama, *Catal. Rev.-Sci. Eng.*, **1988**, *30*, 249-280.
2. M. A. Pena and L. L. Fierro, *Chem. Rev.*, **2001**, *101*, 1981-2017.
3. G. Gayko, D. Wolf, E. V. Kondratenko and M. Baerns, *J. Catal.*, **1998**, *178*, 441-449.
4. S. H. Lee, D. W. Jung, J. B. Kim and Y.-R. Kim, *Appl. Catal. A*, **1997**, *164*, 159-169.
5. H. Lee, J. C. Jung, H. Kim, Y.-M. Chung, T. J. Kim, S.J. Lee, S.-H. Oh, Y. S. Kim and K. Song, *Catal. Lett.*, **2008**, *122*, 281-286.
6. H. Lee, J.C. Jung, H. Kim, Y.-M. Chung, T.J. Kim, S.J. Lee, S.-H. Oh, Y.S. Kim and I.K. Song, *Catal. Commun.*, **2008**, *9*, 1137-1172.
7. M. Brezeanu, L. Patron, I. Mândru, F. Tuna and N. Stănică, *Rev. Roum. Chim.*, **1994**, *49*, 807-812.
8. L. Patron, I. Mândru and G. Marinescu, "Encyclopedia of Nanoscience and Nanotechnology", J. A. Schwarz C. Contescu and K. Putyera, Publisher (Ed.), Marcel Dekker, New York, 2004, p. 1683-1699.
9. B. von Grande, H. K. Muller-Buschbaum and M. Schweizer, *Z. Anorg. Allgem. Chem.*, **1975**, *414*, 76-83.
10. L.-H. Wang, X.-D. Yi, W.-Z. Weng and H.-L. Wan, *Catalysis Today*, **2008**, *131*, 135-139.
11. O. V. Buyevskaya, M. Rothaemel, H. W. Zanthoff and M. Baerns, *J. Catal.*, **1994**, *146*, 346-357.
12. K. Nomura, T. Hayakawa, K. Takehira and Y. Ujihira, *Appl. Catal. A*, **1993**, *101*, 63-72.
13. R. Spinicci, P. Marini, S. De Rossi, M. Faticanti and P. Porta, *J. Mol. Catal., A*, **2001**, *176*, 253-265.